



HAL
open science

Dissolution of Cavities and Porous Media: a Multi-Scale View

Michel Quintard

► **To cite this version:**

Michel Quintard. Dissolution of Cavities and Porous Media: a Multi-Scale View. MAMERN'13: The 5th International Conference on Approximation Methods and Numerical Modelling in Environment and Natural Resources, Apr 2013, Granada, Spain. pp.1-14. hal-04021092

HAL Id: hal-04021092

<https://hal.science/hal-04021092>

Submitted on 9 Mar 2023

HAL is a multi-disciplinary open access archive for the deposit and dissemination of scientific research documents, whether they are published or not. The documents may come from teaching and research institutions in France or abroad, or from public or private research centers.

L'archive ouverte pluridisciplinaire **HAL**, est destinée au dépôt et à la diffusion de documents scientifiques de niveau recherche, publiés ou non, émanant des établissements d'enseignement et de recherche français ou étrangers, des laboratoires publics ou privés.

Dissolution of Cavities and Porous Media: a Multi-Scale View

Michel Quintard^{1,2}

¹Université de Toulouse ; INPT, UPS ; IMFT (Institut de Mécanique des
Fluides de Toulouse) ;
Allée Camille Soula, F-31400 Toulouse, France
quintard@imft.fr

² CNRS ; IMFT ;
F-31400 Toulouse, France

Keywords: Dissolution, Cavity, Porous Media, Non-Equilibrium Models, Wormhol-
ing, Effective Surface.

Abstract. *Dissolution of underground cavities or porous media involves many different scales that must be taken into account in modeling attempts. This paper presents a review of some of these problems. The paper starts with an introduction to non-equilibrium models, which play an important role in understanding dissolution physics for such media. In particular, their fundamental importance in catching dissolution instability diagrams is emphasized. A second multi-scale aspect is the introduction of the concept of effective surface for dealing with heterogeneous and/or rough surfaces. All these concepts may be used to develop efficient large-scale simulations. Examples are given for simple situations which emphasize the strong coupling between dissolution and buoyancy plumes generated within the dissolution boundary layer.*

1 Introduction

Dissolution of underground cavities are found in many fields such as mining of saline formations, karst formation, etc [7, 26]. While dissolution mechanisms are not restricted to natural media, the multiple-scale aspects associated with dissolution are inherent to any geological application. This multiple-scale feature is illustrated in Figure 1 which, in a very schematic manner, presents several aspects associated to the injection of a dissolving fluid in a geological formation (acid injection in petroleum engineering, solution mining, ...) or dissolution through natural water circulation. Typically, one may have the dissolution of a porous medium, which under certain circumstances may lead to a dissolved region with a porosity gradient before a true fluid cavity, or an impervious rock formation with a more direct route to a fluid cavity. Various types of heterogeneity will make the multi-scale feature more complicated. Pore-scale modeling is inaccessible to direct modeling at the cavity scale, and some sort of macro-scale modeling is necessary. Macro-scale models are not necessarily unique, as will be discussed in the next section (discussion about local equilibrium or local non-equilibrium models). Similarly, in the case of a solid rock formation with a sharp dissolving interface, it is often difficult to take into account in a direct manner at the cavity-scale small-scale heterogeneities and/or roughness over the interface. The macro-scale model takes often the form of an effective surface theory, and this point will be discussed later in this paper. Finally, additional intermediate scale features are process dependent, especially the structures induced by dissolution instabilities (wormholing) or coupling between dissolution and hydrodynamic instabilities (notably natural convection and salt fingering). These latter aspects will be discussed in the last section.

2 Porous Media Models

In this section, we discuss the introduction of macro-scale models in a simple case to illustrate the discussion. Suppose the liquid phase, denoted β , is a binary mixture containing species A and B and the solid phase σ contains only species A. The balance equations may be written

$$\frac{\partial \rho_\beta}{\partial t} + \nabla \cdot (\rho_\beta \mathbf{v}_\beta) = 0 \quad (1)$$

$$\frac{\partial (\rho_\beta \omega_{A\beta})}{\partial t} + \nabla \cdot (\rho_\beta \omega_{A\beta} \mathbf{v}_\beta - \rho_\beta D_{A\beta} \nabla \omega_{A\beta}) = 0 \quad (2)$$

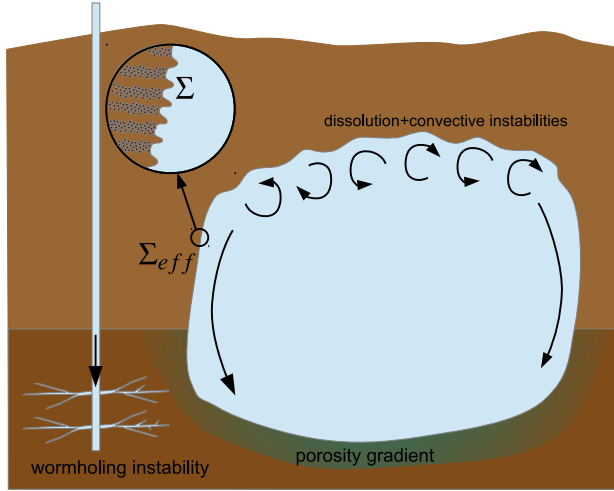


Figure 1: Cavity dissolution: an illustration of various multi-scale problems

where $\omega_{A\beta}$ represents the mass fraction of species A and a similar equation hold for species B. The mass balance equation for the σ -phase is written as

$$\frac{\partial \rho_\sigma}{\partial t} + \nabla \cdot (\rho_\sigma \mathbf{v}_\sigma) = 0 \quad (3)$$

Of course, the problem must be completed by momentum and energy balances. It is often assumed a quasi-steady coupling between the dissolution problem and the other transport problems (i.e., velocity is assumed to be a known field and temperature is nearly uniform over the averaging volume). At the $\beta - \sigma$ interface (denoted by $A_{\beta\sigma}$ in the following text), the chemical potentials for each species should be equal between the different phases and this results in a classical equilibrium condition

$$\omega_{A\beta} = \omega_{Aeq} \quad \text{at } A_{\beta\sigma} \quad (4)$$

The mass balance for species A at the $\beta - \sigma$ interface gives

$$\rho_\beta \omega_{A\beta} (\mathbf{v}_{A\beta} - \mathbf{w}) \cdot \mathbf{n}_{\beta\sigma} = \rho_\sigma \omega_{A\sigma} (\mathbf{v}_{A\sigma} - \mathbf{w}) \cdot \mathbf{n}_{\beta\sigma} \quad \text{at } A_{\beta\sigma} \quad (5)$$

where

$$\rho_\beta \omega_{A\beta} \mathbf{v}_{A\beta} = \rho_\beta \omega_{A\beta} \mathbf{v}_\beta - \rho_\beta D_{A\beta} \nabla \omega_{A\beta} \quad (6)$$

The total mass balance at the $\beta - \sigma$ interface gives

$$\rho_\beta (\mathbf{v}_\beta - \mathbf{w}) \cdot \mathbf{n}_{\beta\sigma} = \rho_\sigma (\mathbf{v}_\sigma - \mathbf{w}) \cdot \mathbf{n}_{\beta\sigma} \quad \text{at } A_{\beta\sigma} \quad (7)$$

where \mathbf{w} represents the velocity of the interface. As $\omega_{B\sigma} = 0$ in the solid phase, we may write

$$\rho_\beta \omega_{A\beta} (\mathbf{v}_{A\beta} - \mathbf{w}) \cdot \mathbf{n}_{\beta\sigma} = \rho_\beta (\mathbf{v}_\beta - \mathbf{w}) \cdot \mathbf{n}_{\beta\sigma} \quad \text{at } A_{\beta\sigma} \quad (8)$$

We have now all in hands to discuss the development of macro-scale models. Pore-scale modeling of dissolution processes [3] shows how complex is the interaction between the various transport processes. In particular, the interface evolution may be very complex and process dependent [19]. One is not surprised that the development of macro-scale models is therefore very difficult. Indeed, one may consider that this is still an open problem, if one considers the historical aspects and complex interactions previously mentioned. Even if one consider a quasi-steady coupling, the problem of active dispersion (dispersion with mass exchange at the interface) is known to lead to various models. In particular, we may develop two classes of model if one looks at the difference between the equilibrium concentration and the average concentration. If this difference is very small, the situation is called local equilibrium, and our simple case leads to a very straightforward macro-scale equation for the concentration

$$\Omega_{A\beta} = \omega_{Aeq} \quad (9)$$

where $\Omega_{A\beta}$ is the intrinsic average mass fraction. The non-equilibrium case may lead to various models, since the exchange may feature non-local in space and time mechanisms. At first order, one may follow the works of [21, 22, 14, 6, 23] to derive a general dissolution equation under the form of

$$\frac{\partial \varepsilon_\beta \rho_\beta \Omega_{A\beta}}{\partial t} + \nabla \cdot (\varepsilon_\beta \rho_\beta \Omega_{A\beta} \mathbf{U}_\beta + \dots) = \nabla \cdot (\varepsilon_\beta \rho_\beta \mathbf{D}_{A\beta}^* \cdot \nabla \Omega_{A\beta}) + K_{\beta\sigma} \quad (10)$$

where ε_β is the fluid volume fraction, \mathbf{U}_β the interstitial velocity, $\mathbf{D}_{A\beta}^*$ the active effective dispersion tensor, and $K_{\beta\sigma}$ the mass exchange term. It is often approximated as

$$K_{\beta\sigma} = -\alpha (\Omega_{A\beta} - \omega_{Aeq}) + \dots \quad (11)$$

The dots in these equations account for additional terms that may be generally written under the form of additional convective terms, thus potentially affecting the front velocity. It is important to acknowledge that, if these terms cannot be neglected, the traditional expression $K_{\beta\sigma} = -\alpha (\Omega_{A\beta} - \omega_{Aeq})$ does not account for all the exchange flux! This has been recognized in some cases, as illustrated in [13]. Another feature that is often ignored by ‘‘common’’ knowledge is that the active dispersion tensor, $\mathbf{D}_{A\beta}^*$, is not necessarily equal to the passive one (i.e., the one with no-flux at $A_{\beta\sigma}$, see for instance illustration in [21]).

How does the various models affect the macro-scale behavior? One example is illustrated in Figure 2. This figure represents the dissolution patterns obtained by injection of a dissolving fluid into a homogeneous porous medium. The pictures represent the porosity field (blue=initial porosity, red=dissolved area, i.e., pure fluid) for various injection flow-rates. The curve is the ratio of the injected volume at breakthrough versus the pore volume. The first picture represents a case of local equilibrium dissolution (characterized by a thin dissolution front). The process is stable at low velocity. Increasing the velocity leads to the development of well known unstable dissolution fronts [15, 8, 9, 14]. Increasing the velocity also triggers the appearance of non-equilibrium dissolution regimes, starting with the ramified wormholing regime. These regimes are characterized by thick dissolution fronts over which porosity varies continuously. It is very interesting to find that the dissolution front may be stable again at very high velocity, because of the non-equilibrium mechanisms.

The dominant wormhole regime is used in petroleum engineering to bypass low permeability areas near well-bores. How to find the optimal conditions? It was shown in [14] that the optimal condition is found at the junction between the dominant wormhole, local equilibrium dissolution pattern and the ramified wormhole, local non-equilibrium pattern. This illustrates the interest of non-equilibrium models for describing dissolution processes. Another interest of non-equilibrium dissolution models is the fact that their represent a diffuse interface model for dissolution and can be used to model fluid/solid cavity dissolution problems as illustrated and discussed in [18], without explicit treatment of the interface.

3 Effective Surface modeling

Another interesting multi-scale aspect associated to dissolution problem is the fact that, often, the dissolving surface is heterogeneous as it is illustrated in Figure 3.

The top drawings in this figure represent the dissolution history of the actual surface of a stratified medium, subjected to a chemical reaction with a first order reaction rate which depends on the material. Generally, depending on the Damköhler numbers, the receding surface velocity variations create roughnesses. For some boundary conditions for the large-scale problems, the surface roughness becomes quasi-steady and the receding velocity becomes a constant. This receding velocity depends on the roughnesses and the flow conditions [25]. One understands that catching this local behavior requires solving the transport equations at this scale, which is in general orders of magnitude lower than the process scale (cavity, well, ...). Therefore, it is interesting to

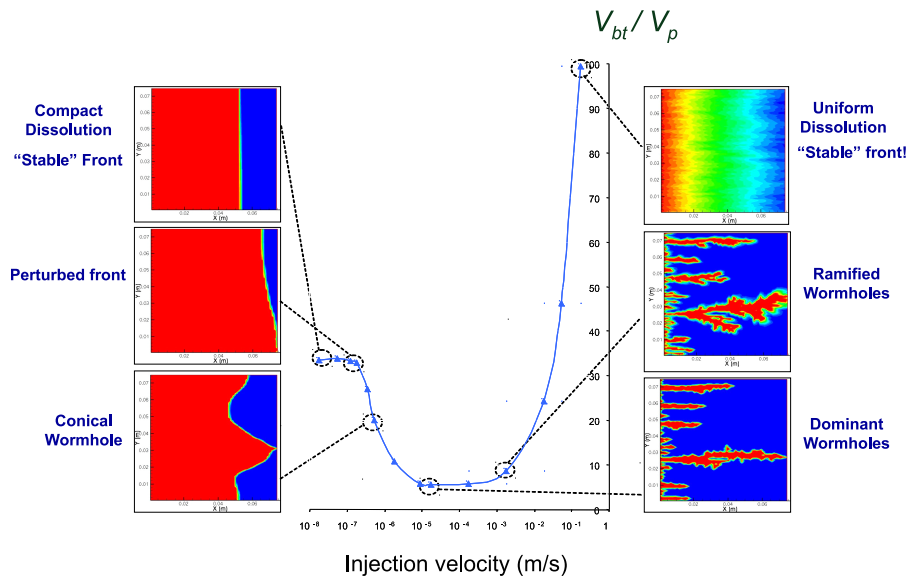


Figure 2: Diagram of dissolution patterns for injection of a dissolving fluid in a porous medium (after [5] work)

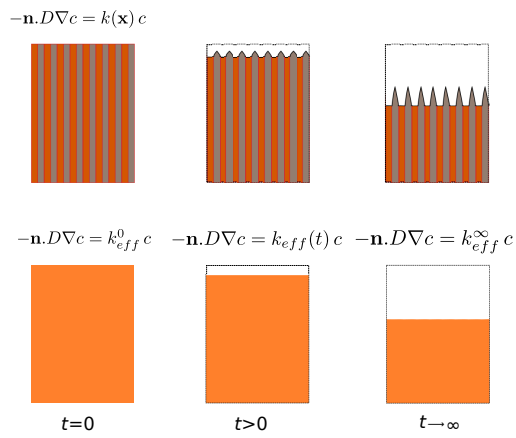


Figure 3: Real surface dissolution history and the illustration of the concept of effective surface.

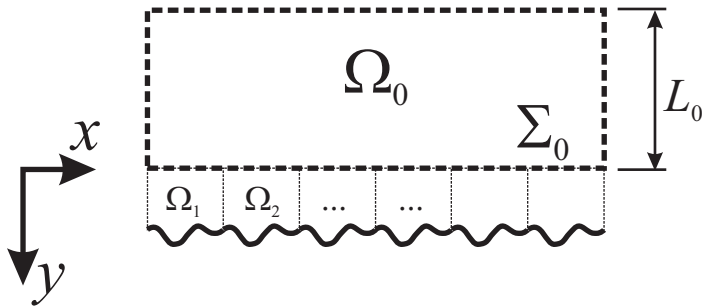


Figure 4: The domain decomposition method

investigate the possibility of replacing this heterogeneous, rough surface by a smooth, homogenous effective surface. The equivalence criterion is essentially the obtainment of the same receding velocity. Given the transient nature of the dissolution of such heterogeneous, rough surfaces, several questions must be solved:

- where to put the surface,
- which effective boundary condition to apply at the effective surface?

The case without dissolution has received a lot of attention especially for the case of Navier-Stokes equations over the rough surface [1, 2, 20, 24, 17]. The technique to derive effective surface and boundary conditions is generally based on a decomposition method, as illustrated in Fig. 4, with a bulk volume where the original equations are solved and unit-cell small regions over the surface where the solution of the transport equations is sought under the form of a deviation to a n-th order continuation of the bulk solution. In the case of Navier-Stokes equations, for an arbitrary position of the effective surface, the effective surface boundary condition has the form of a Navier condition. Using Taylor's expansion one can change easily the position of the effective surface, which will also change the effective surface boundary condition. For the Navier-Stokes equations, it is possible to determine the position at which the Navier condition reverts to the no-slip condition.

Figure 5 illustrates the concept of effective surface. The top drawing represents the actual problem, here the development of a boundary layer over a rough surface. The bottom figure represents the effective surface treatment, with the effective surface positioned at the place which gives the no-slip condition.

For a reactive surface, without dissolution, it was found that, for a given position of the effective surface, the effective boundary condition is a first order

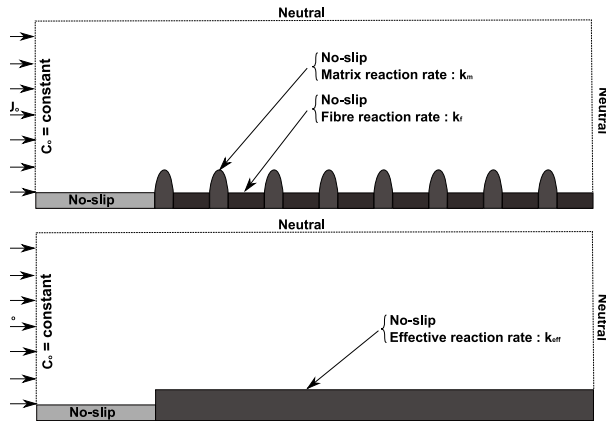


Figure 5: Illustration of the concept of effective surface

reaction rate condition, but with an effective reaction rate that depends on the actual reaction rates, the roughnesses and flow conditions, as well as the effective surface position. An example of calculation is plotted Figure 6, which represents the ratio of the effective reaction rate over the surface average of the point reaction rate, versus the mean value of the surface Damkhöler number, for various unit cell geometry. For small Damkhöler numbers, the effective reaction rate is equal to the surface average, k_{av} defined by the surface integral of k over the surface divided by the projected surface. This can be explained by the fact that, in this case, the concentration near the surface is almost constant, thus giving a flux proportional to the point reaction rate. This ratio tends to decrease with increasing Damkhöler numbers. For very large Damkhöler numbers, the concentration is almost zero along the surface. K_{eff} becomes a constant, which is equal to the surface harmonic average in the case of a flat surface, denoted k_h .

The picture becomes a little bit more complicated if one takes into account the surface evolution with dissolution [25]. If we start with a flat surface:

- the initial effective reaction rate will be the surface arithmetic average,
- after a transient evolution, the surface recession velocity becomes a constant with an effective reaction rate equal to the maximum point reaction rate. In fact, the surface roughness adapts to the heterogeneity with a recession velocity determined by the weakest (i.e., the highest reaction rate) material. The ratio of the reaction rates will determine the roughness itself, but not the recession velocity!

For very large Damkhöler numbers, the picture is different: the surface remains

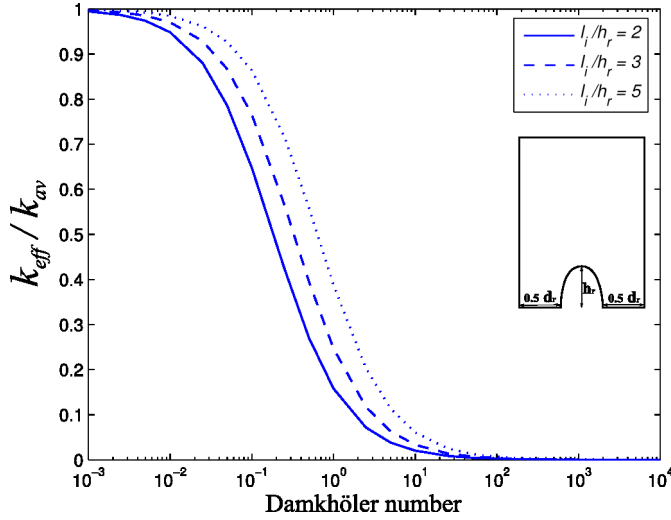


Figure 6: Effective reaction rate as a function of the Damkhöler number (from[24])

flat and the effective reaction rate is equal to k_h . For intermediate cases, the roughness evolution and the associated effective reaction rate is complex and, so far, must be determined experimentally or numerically.

4 Dissolution Structures

At this point, length-scales have been determined initially by the material and domain properties. When studying the concept of effective surface, we already have seen that the surface roughness, while staying of the same order as the original heterogeneity, becomes process dependent. This is such that no a priori effective surface theory may be used without computing the surface geometry evolution. The introduction of process dependent scales in the analysis is often required when considering the existence of instabilities. In this section, we will consider two types of instabilities:

- Dissolution instabilities: the dissolution process is at the core of the instability onset,
- Coupling between classical hydrodynamic instabilities such as convective patterns and dissolution.

The impact of dissolution instabilities has been the object of discussion in Sec. 2. Figure 2 shows that small scales can be created through the development of dissolution instabilities, and this is still an open problem to develop efficient numerical methods to obtain the wormholing dynamic for domains of

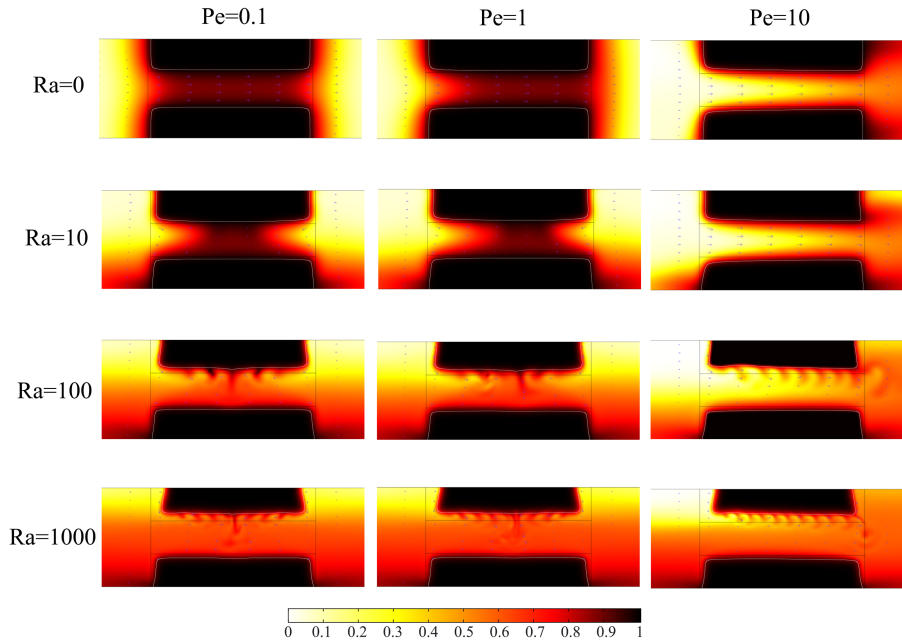


Figure 7: Dissolution of a tube for various Péclet and Rayleigh numbers (from [18])

industrial scales. Attempts have been made to develop averaged models incorporating the wormhole dynamics, or other instability patterns, and we refer the reader to some literature on the subject to understand the different estimates and possibilities that have been explored [11, 12, 4].

Coupling with hydrodynamic instabilities is another complex, and still open, problem. While coupling with inertial flow vortices is also a very important question, a typical hydrodynamic instability that often plays a very important role is natural convection arising from density variations with concentration. This is quite inevitable and typical for salt cavities [10]. Figure 7 shows the dissolution of a tube for various Péclet and Rayleigh numbers, as obtained numerically by [18].

The interpretation is the following:

- for small Rayleigh and Péclet numbers, the concentration gradients are relatively small within the tube and the concentration field is symmetric. As a consequence, the dissolution is symmetric and the tube wall slope small,
- for small Rayleigh numbers, if we increase the Péclet number, convec-

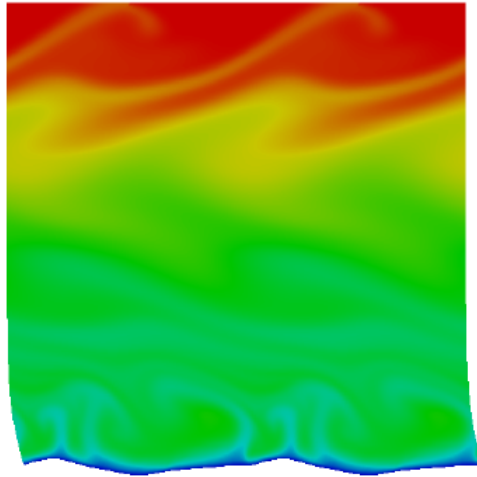


Figure 8: Corium-Concrete interaction, close-up near the surface showing the formation of cup-shaped structures (work of [16])

tive boundary layers tend to develop, the flow remains symmetric but the slope wall become large,

- for small Péclet numbers, if we increase the Rayleigh number, natural convection starts to play a role, with convective “rolls” of smaller length-scales as the Rayleigh number increases. The flow becomes non-symmetric, hence the dissolving surface, with, for this particular situation, a relatively flat surface at the bottom and a more rough surface at the top where the “salt fingers” are initiated.
- for large Rayleigh numbers, if we increase the Péclet number, the instabilities are flushed away, with a tendency to decrease the roughness of the dissolved wall.

Depending on the geometry of the system, the interaction between the hydrodynamic instabilities and the dissolution process may produce different surface patterns. If the surface is initially flat and horizontal, a typical cup-shaped structure is generated, as illustrated in Figure 8, which is taken from the work of [16] who explored the interaction between concrete walls and Corium, in the framework of nuclear reactor severe accident studies.

5 Conclusion

In this paper, the emphasis has been put on the various models that can be developed at the different scales characteristic of dissolution problems, pore-scale to Darcy-scale models, the concept of effective surface, and the consequences of these models especially in terms of dissolution instabilities or coupling between dissolution and hydrodynamic instabilities. These latter effects create additional intermediate scales which contribute to the complexity of dissolution problems.

The emphasis has been put here on theoretical aspects. Of course, many other aspects are equally important and have received significant contributions in the past decades: experimental characterization of transport properties or large-scale dissolution patterns, pore-scale tomographic observations, dissolution morphology, etc...

Acknowledgements

This review incorporates the contribution of many PhD students and collaborators, as well as many supporting institutions or companies. This information can be collected from the various references cited in this paper.

REFERENCES

- [1] Y. Achdou, P. Le Tallec, F. Valentin, and O. Pironneau. Constructing wall laws with domain decomposition or asymptotic expansion techniques. *Computer Methods in Applied Mechanics and Engineering*, 151(1-2):215–232, 1998.
- [2] Y. Achdou, O. Pironneau, and F. Valentin. Effective boundary conditions for laminar flows over periodic rough boundaries. *Journal of Computational Physics*, 147(1):187–218, 1998.
- [3] S. Bekri, J. F. Thovert, and P. M. Adler. Dissolution of porous media. *Chem. Engng Sci.*, 50:2765–2791, 1995.
- [4] C. E. Cohen, D. Ding, M. Quintard, and B. Bazin. A large scale dual-porosity approach to model acid stimulation in carbonated reservoir. In *10th European Conference on the Mathematics of Oil Recovery, ECMOR X*, volume paper B038, pages 1–9, Amsterdam, 2006.
- [5] C. E. Cohen, D. Ding, M. Quintard, and B. Bazin. From pore scale to wellbore scale: Impact of geometry on wormhole growth in carbonate acidization. *Chemical Engineering Science*, 63(12):3088–3099, 2008.

- [6] F. A. Coutelieris, M. E. Kainourgiakis, A. K. Stubos, E. S. Kikkinides, and Y. C. Yortsos. Multiphase mass transport with partitioning and inter-phase transport in porous media. *Chemical Engineering Science*, 61(14):4650–4661, 2006.
- [7] D.C. Ford and P. Williams. *Karst Hydrogeology and Geomorphology*. Wiley, 2007.
- [8] C. N. Fredd and H. S. Fogler. Influence of transport and reaction on wormhole formation in porous media. *AIChE Journal*, 44(9):1933–1949, 1998.
- [9] C. N. Fredd and H. S. Fogler. Optimum conditions for wormhole formation in carbonate porous media: Influence of transport and reaction. *SPE Journal*, 4(3):196–205, 1999.
- [10] D. Gechter, P. Huggenberger, P. Ackerer, and H. N. Waber. Genesis and shape of natural solution cavities within salt deposits. *Water Resources Research*, 44(11):1–18, 2008.
- [11] F. Golfier, B. Bazin, R. Lenormand, and M. Quintard. Core-scale description of porous media dissolution during acid injection - part i: Theoretical development. *Computational and Applied Mathematics*, 23(2-3):173–194, 2004.
- [12] F. Golfier, M. Quintard, B. Bazin, and R. Lenormand. Core-scale description of porous media dissolution during acid injection - part ii: Calculation of the effective properties. *Computational and Applied Mathematics*, 25(1):55–78, 2006.
- [13] F. Golfier, M. Quintard, and S. Whitaker. Heat and mass transfer in tubes: An analysis using the method of volume averaging. *J. Porous Media*, 5:169–185, 2002.
- [14] F. Golfier, C. Zarcone, B. Bazin, R. Lenormand, D. Lasseux, and M. Quintard. On the ability of a darcy-scale model to capture wormhole formation during the dissolution of a porous medium. *Journal of Fluid Mechanics*, 457:213–254, 2002.
- [15] M.L. Hoefner and H. S. Fogler. Pore evolution and channel formation during flow and reaction in porous media. *AIChE Journal*, 34(1):45–54, 1988.

- [16] C. Introïni. *Interaction entre un fluide à haute température et un béton : contribution à la modélisation des échanges de masse et de chaleur*. PhD thesis, Université de Toulouse, 2010.
- [17] C. Introïni, M. Quintard, and F. Duval. Effective surface modeling for momentum and heat transfer over rough surfaces: Application to a natural convection problem. *Int. J. Heat Mass Transfer*, 54:3622–3641, 2011.
- [18] H. Luo, M. Quintard, G. Debenest, and F. Laouafa. Properties of a diffuse interface model based on a porous medium theory for solid–liquid dissolution problems. *Computational Geosciences*, 16(4):913–932, 2012.
- [19] L. Luquot and P. Gouze. Experimental determination of porosity and permeability changes induced by injection of co2 into carbonate rocks. *Chemical Geology*, 265:148–159, 2009.
- [20] A. Mikelić and V. Devigne. Ecoulement tangentiel sur une surface rugueuse et loi de Navier. *Annales Mathématiques BLAISE PASCAL*, 9:313–327, 2002.
- [21] M. Quintard and S. Whitaker. Convection, dispersion, and interfacial transport of contaminants: Homogeneous porous media. *Advances in Water resources*, 17:221–239, 1994.
- [22] M. Quintard and S. Whitaker. Dissolution of an immobile phase during flow in porous media. *I&EC Research*, 38(3):833–844, 1999.
- [23] C. Soullaine, G. Debenest, and M. Quintard. Upscaling multi-component two-phase flow in porous media with partitioning coefficient. *Chem Eng Sci*, 66:6180–6192, 2011.
- [24] S. Veran, Y. Aspa, and M. Quintard. Effective boundary conditions for rough reactive walls in laminar boundary layers. *International Journal of Heat and Mass Transfer*, 52:3712–3725, 2009.
- [25] G. L. Vignoles, Y. Aspa, and M. Quintard. Modelling of carbon-carbon composite ablation in rocket nozzles. *Composites Science and Technology*, 70:1303–1311, 2010.
- [26] Jo De Waele, Lukas Plan, and Philippe Audra. Recent developments in surface and subsurface karst geomorphology: An introduction. *Geomorphology*, 106(1–2):1 – 8, 2009.